Supplementary Materials

Synergistic Fe dopant and Co vacancy in CoOOH for enhanced oxygen evolution reaction

Xiaoyi Dou[1], Kepeng Song[2], Riming Hu[3], Mingjin Cui[1], Porun Liu[4], Ziyi Xu[5], Ding Yuan[1], Huakun Liu[1], Shixue Dou[1], Yuhai Dou[1]

[1]Institute of Energy Materials Science, University of Shanghai for Science and Technology, Shanghai 200093, China.
[2]School of Chemistry and Chemical Engineering, State Key Laboratory of Crystal Materials, Shandong University, Jinan 250100, Shandong, China.
[3]Institute for Smart Materials and Engineering, University of Jinan, Jinan 250022, Shandong, China.
[4]Centre for Catalysis and Clean Energy, Gold Coast Campus, Griffith University, Gold Coast 4222, Australia.
[5]State Key Laboratory of Powder Metallurgy, Powder Metallurgy Research Institute, Central South University, Changsha 410083, Hunan, China.

Correspondence to: Prof. Ding Yuan, Institute of Energy Materials Science, University of Shanghai for Science and Technology, Shanghai 200093, China. E-mail: d_yuan@usst.edu.cn

ORCID: Ding Yuan (0000-0002-5432-6378)

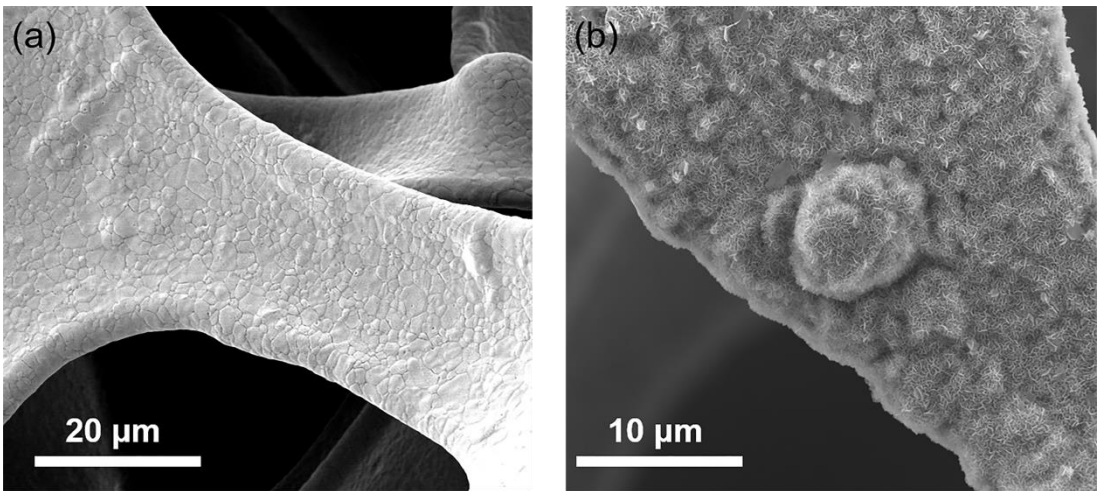

Supplementary Figure 1. SEM images. A: Ni foam (NF); B: $Co(OH)_2$-Fe_D-Co_V/NF.

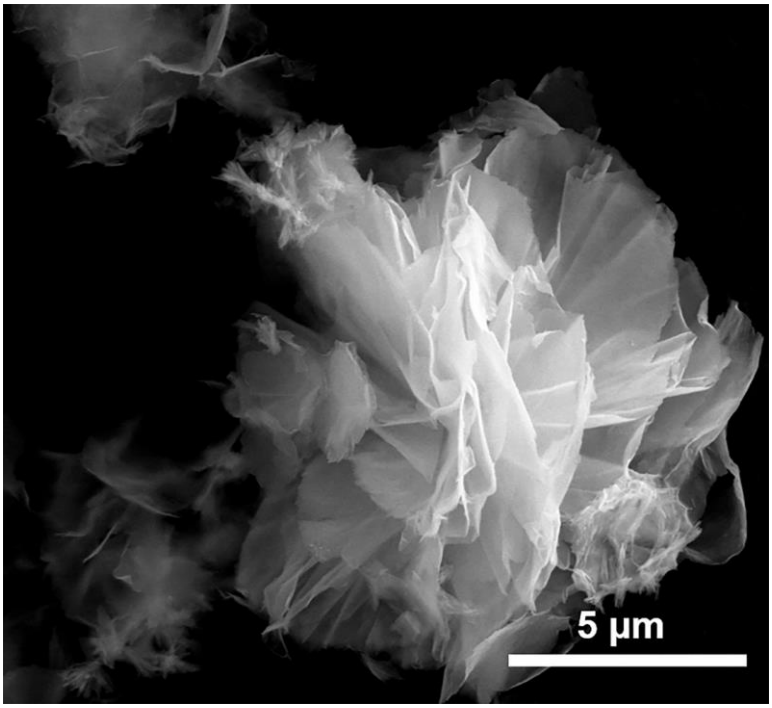

Supplementary Figure 2. SEM images of $Co(OH)_2$-Fe_D-Co_V.

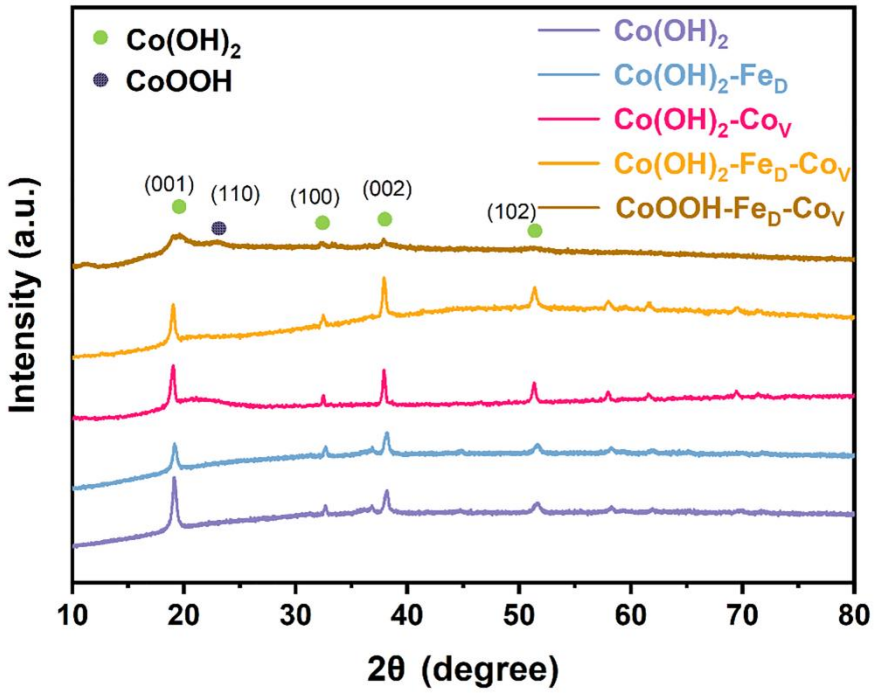

Supplementary Figure 3. XRD patterns of the precursor catalysts and CoOOH-Fe_D-Co_V.

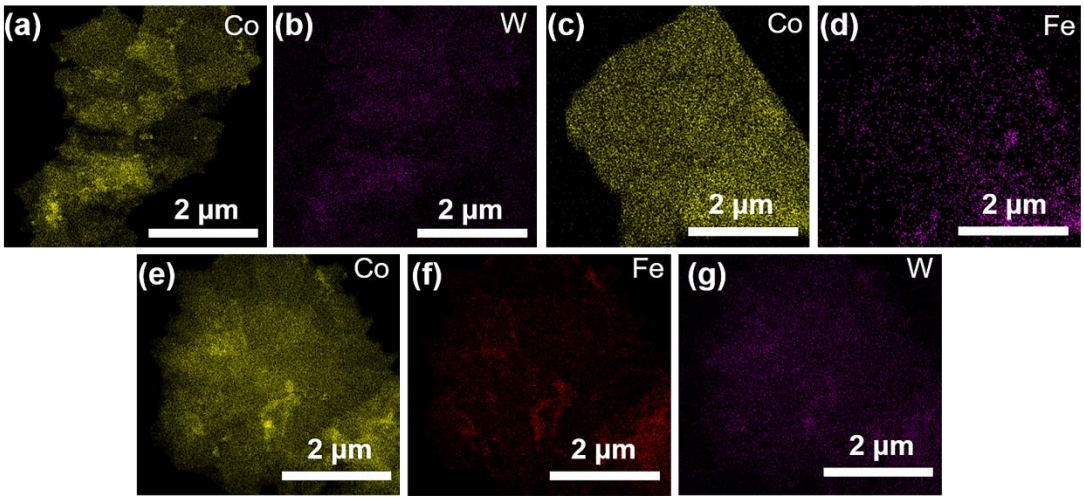

Supplementary Figure 4. EDS spectrum. A-B: CoOOH-Co_V; C-D: $Co(OH)_2$-Fe_D. (e-g) $Co(OH)_2$-Fe_D-Co_V.

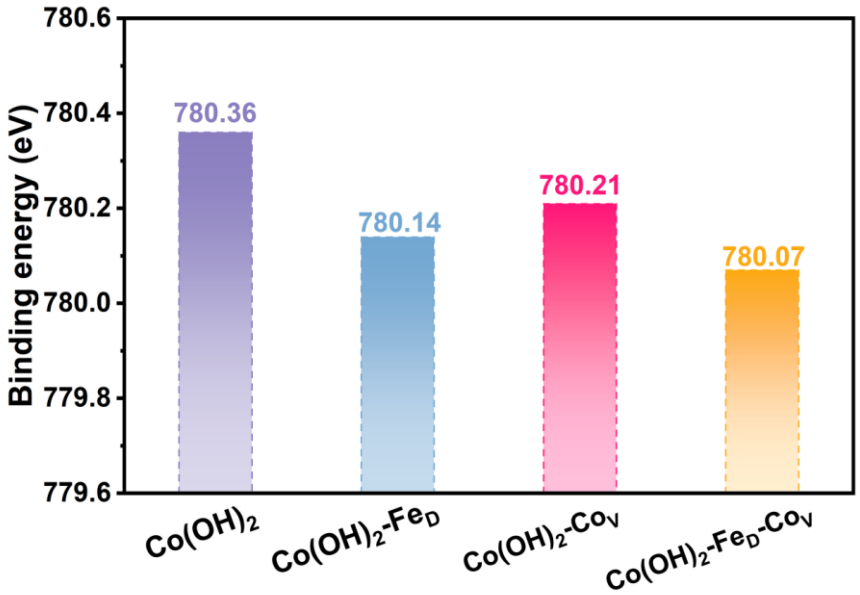

Supplementary Figure 5. Binding energy shift of Co 2p3/2 peak in precursor catalysts.

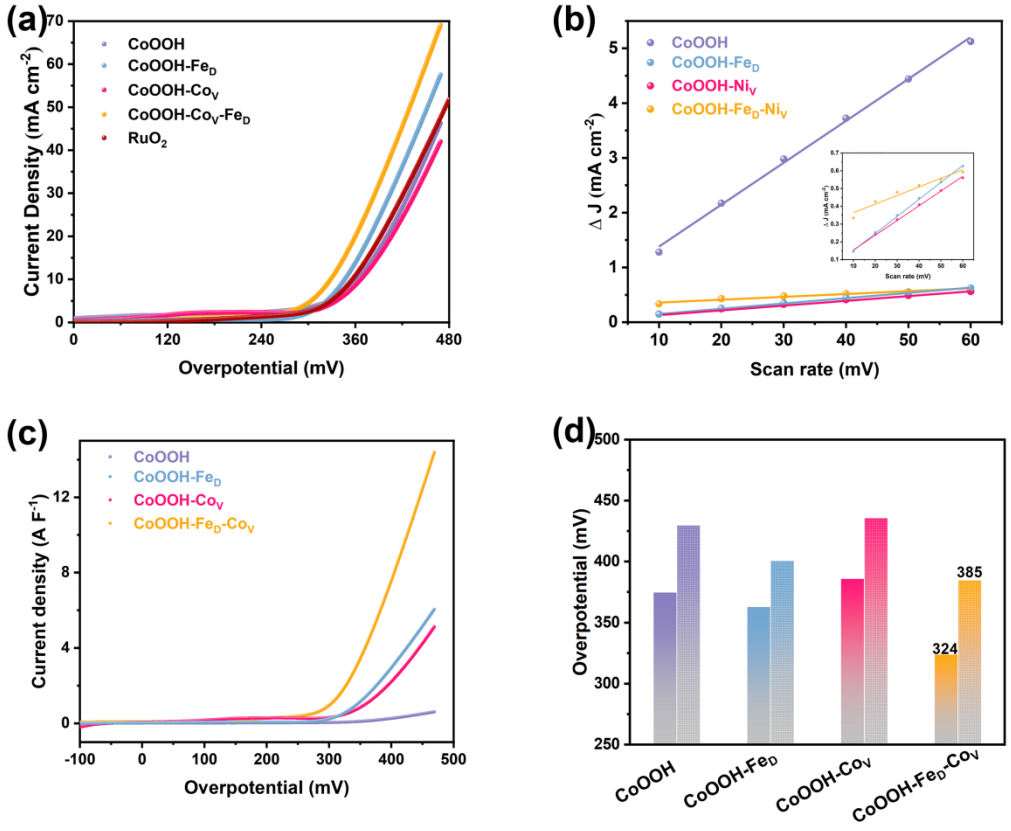

Supplementary Figure 6. OER activity evaluation of catalysts deposited on GCE. A: LSV curves with 80% iR-compensation; B: Differences in current density at 0.25 V vs. Hg/HgO plotted against scan rates and the estimated C_{dl}; C: LSV curves normalized by C_{dl}; D: Overpotentials required to reach 30 mA cm^{-2} of in-situ catalysts (left side) and catalysts deposited on GCE (right side).

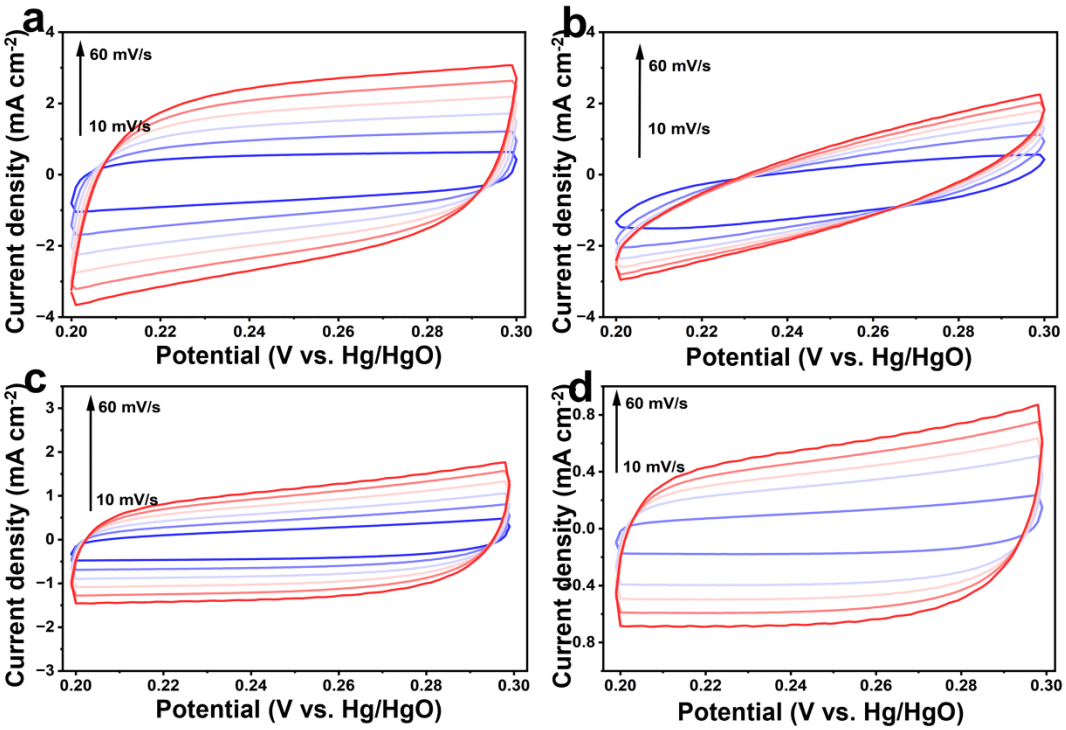

Supplementary Figure 7. Double-Layer capacitance tests. CV curves of A: NiOOH/NF; B: NiOOH-Fe_D/NF; C: NiOOH-Ni_V/NF; D: NiOOH-Fe_D-Ni_V/NF at various scan rates (10-60 mV/s) under the non-Faradaic region.

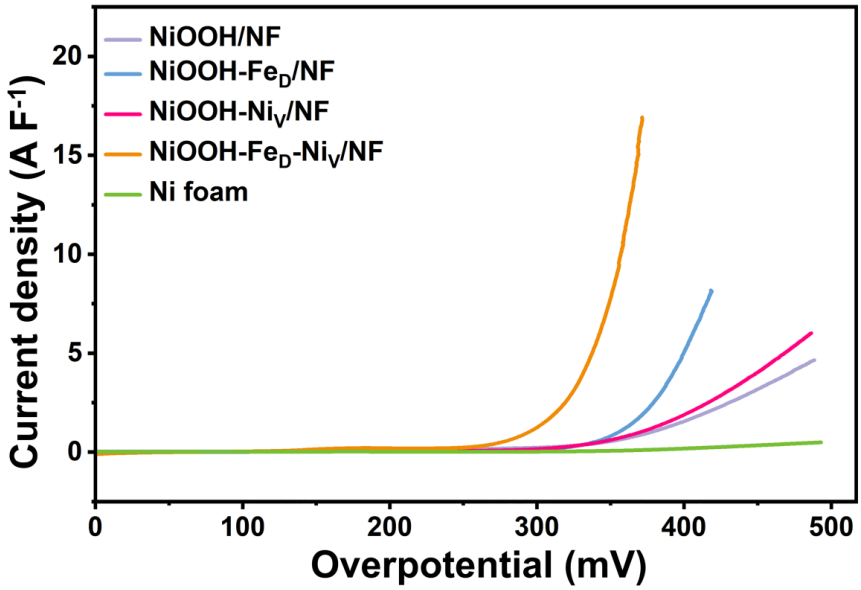

Supplementary Figure 8. LSV curves normalized by C_{dl} (Supplementary Figure 7).

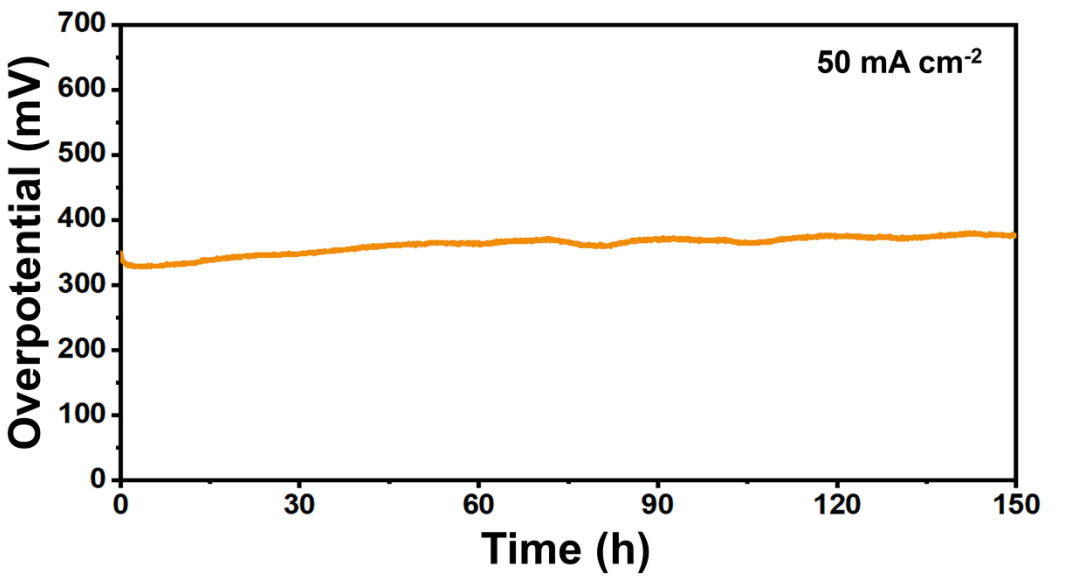

Supplementary Figure 9. Durability evaluation via Amperometric i-t curve test of NiOOH-Fe_D-Ni_V/NF at j = 50 mA cm^{-2} for 150 h.

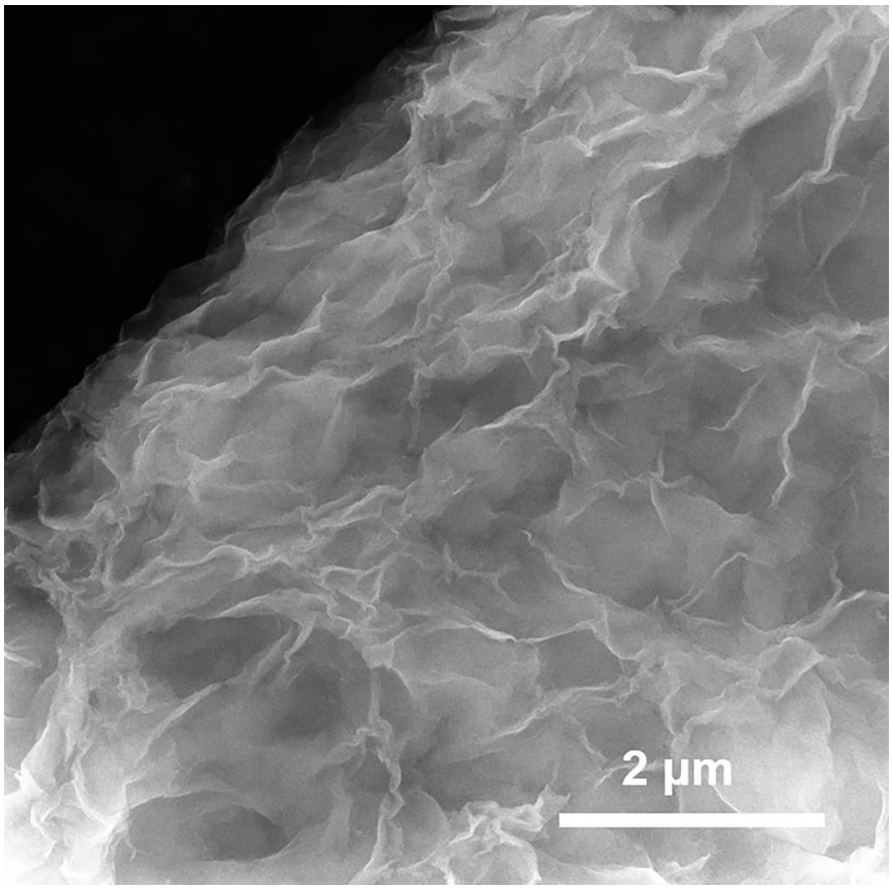

Supplementary Figure 10. SEM image of CoOOH-Fe_D-Co_V ultrasonicationed from the NF-supported CoOOH-Fe_D-Co_V catalyst after durability test.

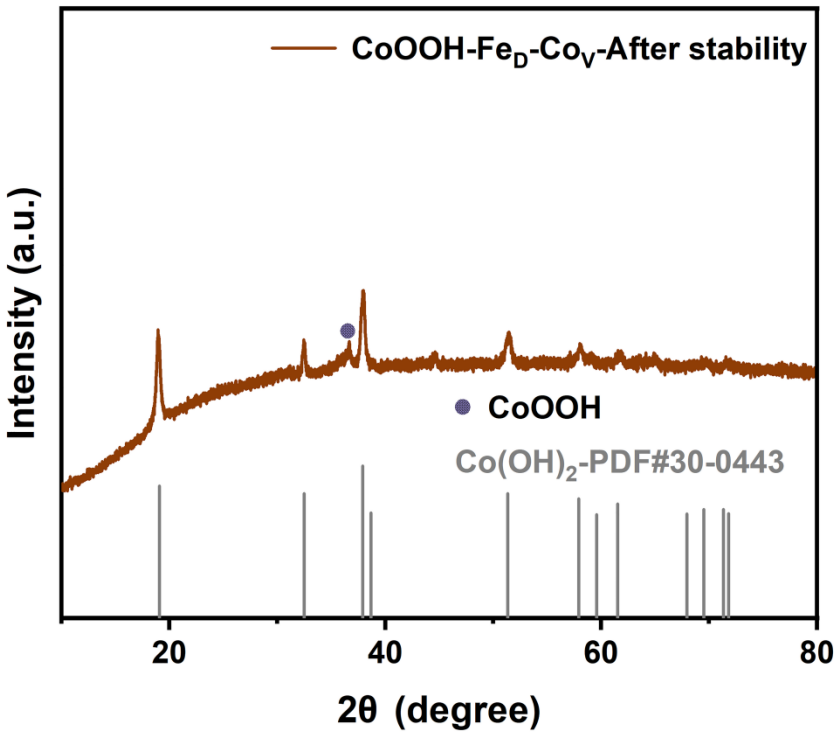

Supplementary Figure 11. XRD pattern of CoOOH-Fe$_D$-Co$_V$ ultrasonicationed from the NF-supported CoOOH-Fe$_D$-Co$_V$ catalyst after durability test.

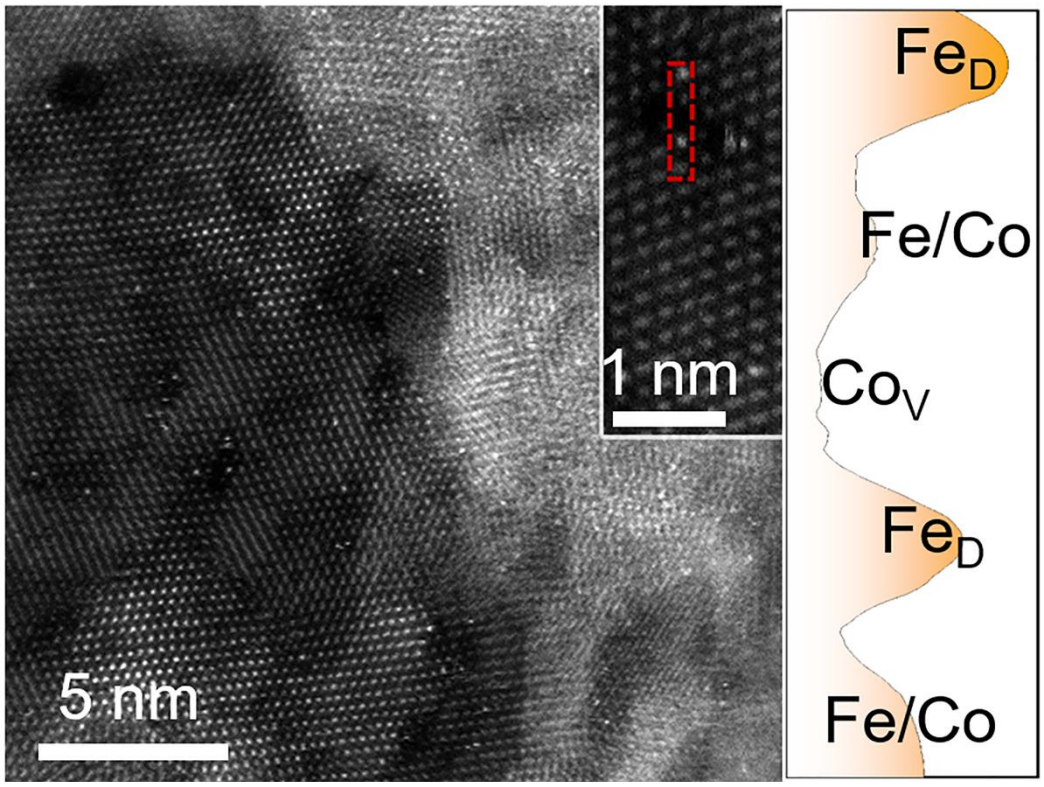

Supplementary Figure 12. HAADF-HRSTEM image and intensity profile of CoOOH-Fe$_D$-Co$_V$ ultrasonicationed from the NF-supported CoOOH-Fe$_D$-Co$_V$ catalyst after durability test.

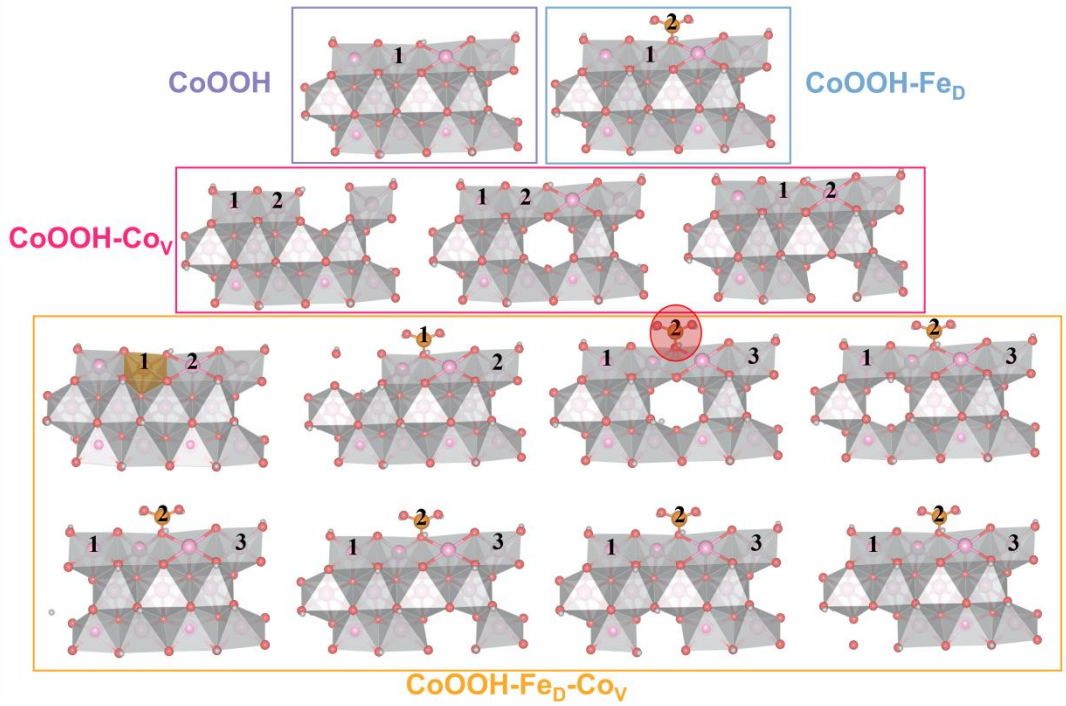

Supplementary Figure 13. Considered active sites of different structure models for DFT calculations.

Supplementary Table 1. Atomic ratios of CoOOH-Fe$_D$, CoOOH-Co$_V$, and CoOOH-Fe$_D$-Co$_V$ obtained from EDX

Atomic Conc. (%) / Catalysts	Co	Fe	W
CoOOH-Fe$_D$	96.75	3.25	/
CoOOH-Co$_V$	99.81	/	0.19
CoOOH-Fe$_D$-Co$_V$	95.03	4.79	0.18

Supplementary Table 2. Peak area ratio of Co with different valence states in different catalysts

$Co^{3+}/(Co^{2+}+Co^{3+})$ Catalyst Catalyst	CoOOH	CoOOH-Fe$_D$	CoOOH-Co$_V$	CoOOH-Fe$_D$-Co$_V$
2p 3/2	30.6	42.4	38.85	63.4
2p 1/2	16.7	11.18	17.2	63.8

Supplementary Table 3. Calculated Gibbs free energy and overpotentials of different metal sites. (The active sites provided below were named from left to right of each structural model provided in Supplementary Figure 10)

	Gibbs free energies (eV)				Gibbs free energy change(eV)				η^{OER} (mV)
	ΔG_{O} $_{H^*}$	ΔG $_{O^*}$	ΔG_{OOH} $_{*}$	Δ G_{O2}	Δ G_1	ΔG_2	ΔG_3	ΔG_4	
CoOOH-Co	0.62	2.3	3.92	4.92	0.6	1.74	1.56	1.00	510
CoOOH-Fe$_D$-Co	0.84	2.2	3.94	4.92	0.8	1.44	1.66	0.98	430
CoOOH-Fe$_D$-Fe	0.98	2.2	4.02	4.92	0.9	1.23	1.81	0.90	580
1-CoOOH-Co$_V$-Co$_1$	0.63	2.3	4.03	4.92	0.6	1.73	1.67	0.89	500
1-CoOOH-Co$_V$-Co$_2$	1.23	2.0	4.28	4.92	1.2	0.79	2.23	0.64	103
2-CoOOH-Co$_V$-Co$_1$	0.88	2.4	3.98	4.92	0.8	1.55	1.55	0.94	320
2-CoOOH-Co$_V$-Co$_2$	1.48	3.3	4.68	4.92	1.4	1.83	1.37	0.24	600

3-CoOOH-Co_V-Co_1	1.18	2.8	4.10	4.92	1.1	1.66	1.26	0.82	430
3-CoOOH-Co_V-Co_2	0.92	2.3	4.04	4.92	0.9	1.45	1.67	0.88	440
1-CoOOH-Fe_D-	0.90	2.4	4.05	4.92	0.9	1.59	1.56	0.87	360
1-CoOOH-Fe_D-	0.64	2.1	3.72	4.92	0.6	1.50	1.58	1.20	350
2-CoOOH-Fe_D-	1.46	2.8	4.43	4.92	1.4	1.39	1.58	0.49	350
2-CoOOH-Fe_D-	1.05	2.8	4.14	4.92	1.0	1.83	1.26	0.78	600
3-CoOOH-Fe_D-	1.07	2.2	4.16	4.92	1.0	1.18	1.91	0.76	680
3-CoOOH-Fe_D-	**0.83**	**2.2**	**3.62**	**4.92**	**0.8**	**1.44**	**1.35**	**1.30**	**210**
3-CoOOH-Fe_D-	0.66	2.4	3.95	4.92	0.6	1.76	1.53	0.97	530
4-CoOOH-Fe_D-	0.76	2.3	3.86	4.92	0.7	1.63	1.47	1.06	400
4-CoOOH-Fe_D-	0.79	2.3	3.53	4.92	0.7	1.53	1.21	1.39	300
4-CoOOH-Fe_D-	0.91	2.2	4.07	4.92	0.9	1.31	1.85	0.85	620
5-CoOOH-Fe_D-	0.96	2.5	4.23	4.92	0.9	1.63	1.64	0.69	410
5-CoOOH-Fe_D-	1.06	2.5	3.97	4.92	1.0	1.44	1.47	0.95	240
5-CoOOH-Fe_D-	1.35	2.4	4.17	4.92	1.3	1.08	1.74	0.75	510
6-CoOOH-Fe_D-	1.07	2.2	4.12	4.92	1.0	1.15	1.90	0.80	630
6-CoOOH-Fe_D-	0.76	2.3	3.64	4.92	0.7	1.55	1.33	1.28	320
6-CoOOH-Fe_D-	0.61	2.3	3.76	4.92	0.6	1.78	1.37	1.16	550
7-CoOOH-Fe_D-	1.07	2.2	4.13	4.92	1.0	1.15	1.91	0.79	490
7-CoOOH-Fe_D-	0.75	2.3	3.68	4.92	0.7	1.55	1.38	1.24	320
7-CoOOH-Fe_D-	0.62	2.3	3.76	4.92	0.6	1.76	1.38	1.16	530
8-CoOOH-Fe_D-	0.94	2.2	4.13	4.92	0.9	1.26	1.93	0.79	700
8-CoOOH-Fe_D-	0.84	2.4	3.91	4.92	0.8	1.59	1.48	1.01	360
8-CoOOH-Fe_D-	0.70	2.4	3.95	4.92	0.7	1.77	1.48	0.97	540